24th COBEM - 2017

24th ABCM International Congress of Mechanical Engineering
December 3-8, 2017, Curitiba, PR, Brazil

COBEM-2017-2698
EXPERIMENTAL MEASUREMENT OF THE ELECTRO MECHANICAL PARAMETERS OF AN ENERGY HARVESTING SYSTEM USING CANTILEVER BEAM

Rafael de Matos Moraes
Niederauer Mastelari
Departamento de Sistemas Integrados, Faculdade de Engenharia Mecânica - UNICAMP, Rua Mendeleyev, 200 - CEP 13083-860
moraerd@fem.unicamp.br
niede@fem.unicamp.br

Abstract. *Harvesting ambient energy provides an opportunity to enable self-powered sensors and instrumentation for big structures such as bridges or petroleum risers. Thus, is increasing the interest for harvest devices of mechanical vibration energy. They are an attractive alternative for removable batteries in these structures, avoiding high cost riskly maintenances, increasing the life time and reliability of structural monitoring systems. Among harvest mechanical sources the piezoelectric conversion principle offers the simplest approach, because there is no need for having complex geometries and mechanisms. By this technic, vibrations are directly converted into electricity through the piezoelectric devices. This work presents a cantilever beam in which has been assembled piezoelectric device. This simple structure has been used for harvest energy study purposes, and has modeled as a mass-spring-damper system operating at first resonance frequency. By this experimental arrangement, it has been possible validate the model, checking if the theoretical calculations have been according the experimental results. The objective has get main electrical and mechanical system parameters of a commercial harvester, such as stiffness of the piezoelectric material, piezoelectric output capacitance, electromechanical coupling factor, natural frequency and damping rate. This knowledge is important to design suitable electronic circuits that match impedances of harvest energy device with power storage device getting maximum efficiency. Electronic Circuit designs and measurement results are presented. The main scope of this work is the development of an interface circuit, an accurate electrical equivalent model of the harvester.*

Keywords: *Energy Harvesting, cantilever beam, power harvester.*

1. INTRODUCTION

Energy harvesters are able to convert ambient energy into usable electrical energy for electronic devices that monitors structures, systems, weather and others. There are many possible conversion mechanisms such as photovoltaic cells, temperature gradients exploiting the Seebeck effect, radio frequency waves, vibrations or motions (Harb, 2011). Since the Curie's brothers (Curie & Curie, 1880) presented the direct effect of piezoelectricity in a kind of salts, the studies in vibrational harvesting changed drastically. From this, vibrations are directly converted into of electricity through the electrodes of the material used as harvester (Hehn & Manoli, 2015).

From this, authors like (Lynch & Loh, 2006; Sazonov, Pillay, Li, & Curry, 2009) make their studies in structural health monitoring (SHM) systems, and some places where the human intervention must be reduced due the fact that some places are difficult to maintenance, as airplanes wings (Giurgiutiu, Zagrai, & Jing Bao, 2002), pipelines (Peairs, Park, & Inman, 2004) and others.

A piezoelectric power harvester can be designed in a simple way and easily developed as cantilevered beam associated with a piezoelectric material. (Ajitsaria, Choe, Shen, & Kim, 2007; a. Erturk & Inman, 2008; Hehn & Manoli, 2015; Williams & Yates, 1996) assume simplified model for this system, by considering a mass-spring-damper first order system operating at resonance.

When it comes to extract the amount of energy efficiently, it is necessary to understand some parameters present in a harvester, such as structure damping, harvester´s capacitance and electro-mechanical coupling factor. These parameters are necessary to have a more complete electrical model and with that, a better management circuit estimation to improve the energy will be harvested. This paper addresses an experimental investigation of power harvesting performance

harmonically excited for any device that has a PZT layer glued to extract energy, as the author (Santos, Hobeck, & Inman, 2016) describe an analytical modeling for different structures for harvesting energy.

2. MODELLING HERVESTER SYSTEM

Figure 1(a) presents a schematic picture of composite beam instrumented by piezoelectric material glued on both sides used for the power harvesting. Authors like (DuToit, Wardle, & Kim, 2005; A. Erturk & Inman, 2008; Hehn & Manoli, 2015; Kim, Kim, & Kim, 2011; Lallart, Garbuio, Petit, Richard, & Guyomar, 2008; Paula & Barbosa, 2013) proposed this system as a single-degree-of-freedom (SDOF) mass-spring-damper, with a circuit coupled as lumped element to extract energy, connect in parallel of spring and damper Fig. 1(b). It resumes this electro mechanical system, which consists of a seismic mass m suspended on a spring with the stiffness k_s and damper d, due the air resistance and friction. When deformation is applied to this piezoelectric beam, it produces electrical energy, and if it's connected with a charge circuit generates a restoring force F_e caused by and electromechanical feedback.

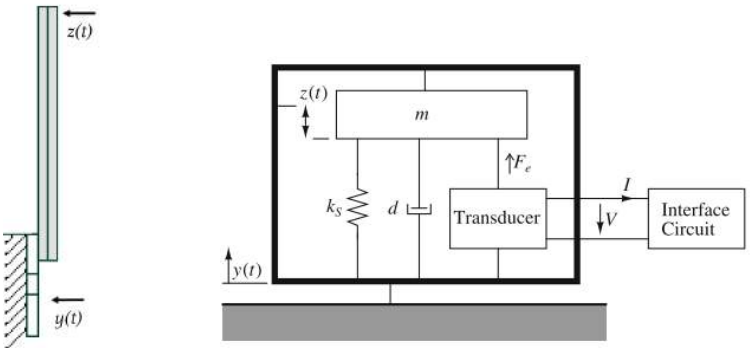

(a) (b)

Figure 1: Model of a kinetic energy harvester connected to lumped elements and a circuit (Source: Hehn and Manoli 2015).

This system in Fig. 1(b) is mathematically modelled by (Hehn & Manoli, 2015):

$$m\ddot{y} = m\ddot{z} + d\dot{z} + k_S z + F_e \tag{1}$$

where $\ddot{z}$, $\dot{z}$, z are the acceleration, velocity and displacement of the beam, m is the mass of harvester, d is the mechanical damping, k_s is the mechanical stiffness and $\ddot{y}$ is the input acceleration.

The constitutive equations of piezoelectric effect as (Rupitsch & Ilg, 2015) and (Hehn & Manoli, 2015) presented are:

$$\begin{cases} S_1 = s_{11}^E T_1 + d_{31} E_3 \\ D_3 = d_{31} T_1 + \varepsilon_{33}^T E_3 \end{cases} \tag{2}$$

where S is mechanical strain, s^E is the compliance under constant electric field, T is mechanical stress, d is the matrix for direct piezoelectric effect, E is the electric field, D is the electrical displacement, ε^T is the dielectric permittivity under constant stress. The constitutive equations of Eq. 2 in terms of F_e, z, V_P and I:

$$\begin{cases} F_e = k_P z + \Gamma V_P \\ I = \Gamma \dot{z} - C_P \dot{V}_P \end{cases} \tag{3}$$

where Γ represents the General Electro-Mechanical Coupling (GEMC) proposed by (Renaud et al., 2008), F_e is the restoring force, k_P is the piezoelectric stiffness, V_P is the electric tension produced, I is the electric current generated and C_P is the piezoelectric capacitance. Substituting F_e of Eq. 1 in 3, it results in Eq. 4.

$$\begin{cases} m\ddot{y} = m\ddot{z} + d\dot{z} + (k_s + k_P) z + \Gamma V_P \\ I = \Gamma \dot{z} - C_P \dot{V}_P \end{cases} \tag{4}$$

The Eq. 4 is described by (Hehn & Manoli, 2015),(Clementino, Reginatto, & Da Silva, 2014),(DuToit et al., 2005).

The GEMC is an interface between mechanical and electrical circuit, and can be associated as a transformer with $1:\Gamma$ ratio. An analogous way of modelling this system, is change to electrical model, and consider mechanical components into electrical domain. High coupling means that a large amount of energy can be harvested from a given environmental

mechanical energy, and this model can be represented as a circuit, where the components are the parameters of the system, show in the Fig. 2.

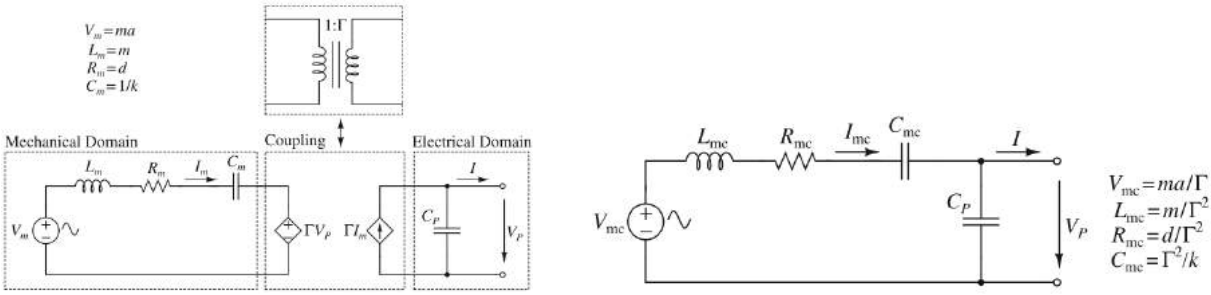

(a) (b)

Figure 2: Equivalent circuit to represent a Kinect energy harvester, (a) with transformer representation, (b) without representation. (Hehn & Manoli, 2015).

For this paper is going to be used the modelling of Fig. 2(b), where V_{mc} is the sinusoidal electric tension, L_{mc} represents the mechanical mass, R_{mc} the mechanical losses or damping and C_{mc} represents the mechanical stiffness and C_P is the piezoelectric capacitance. In order to simplify the circuit, (Ramadass & Chandrakasan, 2010) and (Hehn & Manoli, 2015) proposed a simplification of all the components in Fig. 2(b), to Fig. 3. This model can be considered when an external force is applied at or close the resonant frequency, where C_P and R_P are capacitance and resistance of piezoelectric respectively. R_P is considering also as dielectric losses. This simplification is only valid if a feedback with an interface circuit or an accurate prediction of output power is not necessary. To be more adequate for this study, it is going to be used the model presented in Fig. 2(b).

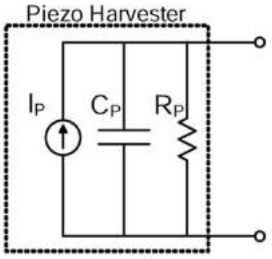

Figure 3: Equivalent circuit with simplification of components (Ramadass & Chandrakasan, 2010).

The harvester can behave capacitively or inductively, as can be seen in the Fig. 4, it depends which frequency it's vibrating. So, it will behave inductively below the resonant and above the anti-resonant frequency. Between these two frequencies, the harvester has capacitively profile. These two frequencies, have some particular characteristics. The first frequency is the resonant, f_r, and the system has minimum impedance. The next frequency is the anti-resonant, f_a, and the system has very high impedance. These frequencies also change mechanical characteristics. So, when the circuit has low impedance, the beam's tip amplitude changes to resonant frequency, and when the impedance is maximum, the frequency is anti-resonant. Once it's interesting to known very well the piezoelectric behavior, it's necessary to define these two frequencies and control the system to be between them. As (Hehn & Manoli, 2015) cited, the load of the circuit coupled to PZT is for f_r, $R = 0$, and for f_a, $R = \infty$.

The piezoelectric capacitance (C_P), it's an internal capacitance presents due the piezoceramics layer. This effect is presented by the existing crystalline structure with the central ion away from middle of structure (tetragonal). Quartz has this characteristic by nature. The most important the polycrystalline ceramics which has this effect is PZT (Lead Zirconate Titanate - $Pb[Zr,Ti]O_2$) and PMN 9 Lead Magnesium Niobate - $Pb[Mg_{1/3}Nb_{2/3}]O_3$). The piezoelectric ceramics have a similar fabrication process of dielectric capacitors, except that have a cooling process to the Curie point while applies a large electric field, this way aligning the poles. (Mason, 2011).

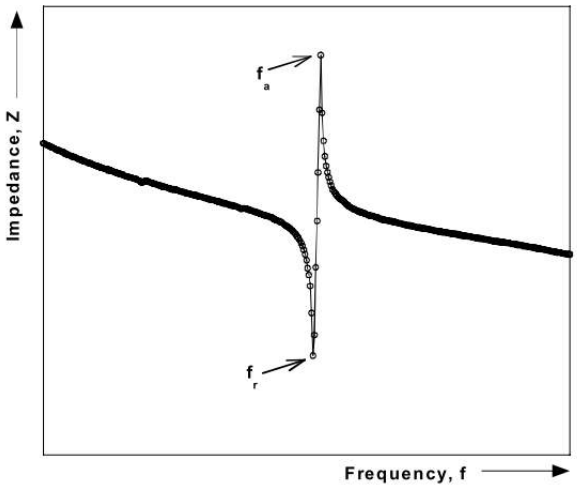

Figure 4: Impedance of piezoelectric (Jordan & Langley, 2001)

The last and not least important factor, is the Electromechanical Coupling Factor. This factor measures the ratio between the mechanical energy applied and the electrical energy converted, it´s an effectiveness indicator. The generic variable used to denote is K_{xy}, where x and y are the directions of applied stress and electric tension created.

$$K_{xy} = \sqrt{\frac{converted\ energy}{input\ energy}} \tag{5}$$

where, in this paper, the converted energy is electrical, and the input energy is mechanical.

This factor has different equations to associate the mode of applied stress and converted energy, if it's below or at resonant frequency, or the shape of piezoelectric. In this paper, could be used for plate shape (Eq. 6), or the generic shape (Eq.7). The associations can be found in (APC International, 2011). For this paper, the electromechanical coupling factor was chosen in Eq. 10, due the missing data available of manufacturer about the PZT beam.

$$K_{31}^2 = \frac{d_{31}^2}{\varepsilon_{33}^T s_{11}^E} \tag{6}$$

$$K_{eff}^2 = \frac{\omega_{OC}^2 - \omega_{SC}^2}{\omega_{OC}^2} \tag{7}$$

The GEMC, was proposed by (Hehn & Manoli, 2015; Renaud et al., 2007, 2008) making an association with the electromechanical coupling factor and GEMC, and then proposed the effective coupling factor in Eq. 8.

$$\Gamma = \sqrt{(K_{eff}^2 * k * C_P)} \tag{8}$$

where k denotes the total stiffness composed by mechanical and piezoelectric material, C_P is the Piezoelectric Capacitance.

As (Clementino, Marcel A.; Junior, Carlos D. M.; Silva, 2013; Hehn & Manoli, 2015; Kong, Ha, Erturk, & Inman, 2010; Vullers, van Schaijk, Doms, Van Hoof, & Mertens, 2009) have cited, to extract more energy efficiently, it's necessary to matching the system's impedance with load impedance. This is also known as Impedance matching. So, the equation o maximum RMS power limit and the resistor maximum power extractable is:

$$P_{Lim} = \frac{(m\hat{a})^2}{8d} \tag{9}$$

$$P_{res} = \frac{(m\hat{a})^2 \omega^2 R_L \Gamma^2}{2\left(\left((k - m + C_P d R_L)\omega^2\right)^2 + \omega^2\left(d + R_L\left(\Gamma^2 + C_P(k - m\omega^2)\right)\right)^2\right)} \tag{10}$$

3. DESCRIPTION OF HARVESTING CANTILEVER

The harvester used in this paper is a commercial beam manufactured by Piezo Systems® and it is a dual layer piezoelectric beam connected in parallel. The piezoelectric beam was coupled to a shaker model K2004E01, and the exciting force was in a base of the beam, as Fig. 5 shows.

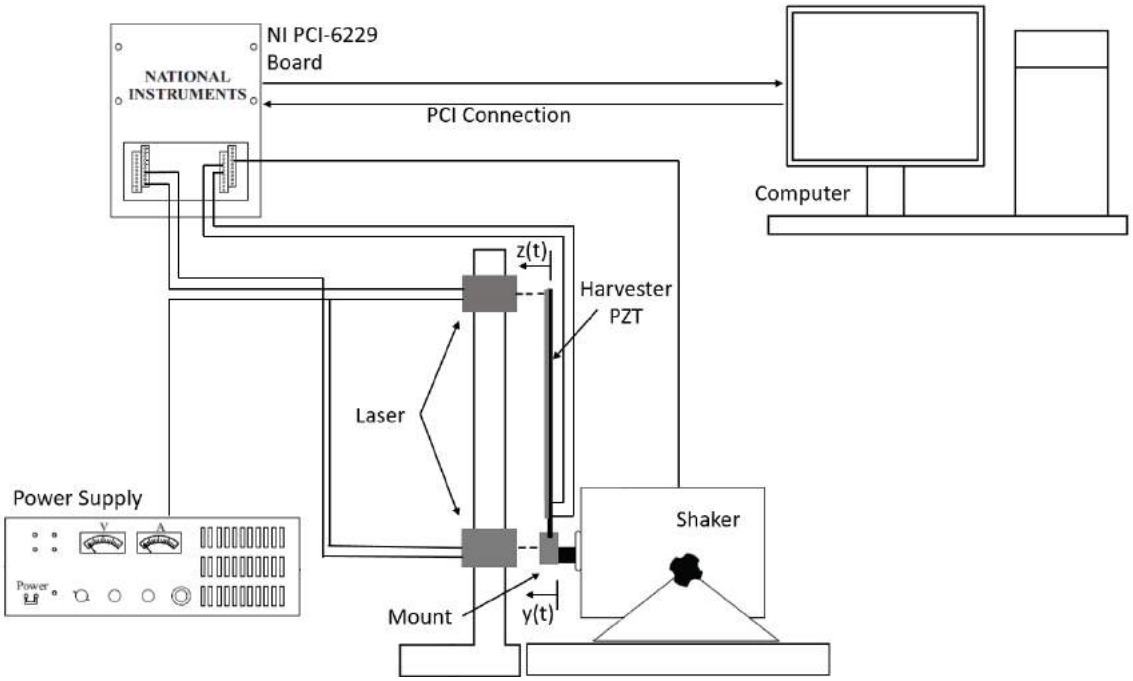

Figure 5: Schematic of experimental setup.

Figure 5 shows the schematic of experimental setup used for instrumentation and collect results. The cantilever piezoelectric beam, is mounted to shaker and applied a sinusoidal input displacement, capable to be measured by the lasers. The Lasers will measure two displacements, y(t) and z(t), or the input displacement given by a shaker and the response of the beam's tip. The data acquisition also is able to acquire the electric tension in PZT terminals.

Some important data are located in Table 1 about the shaker, laser and the acquisition interface board.

Table 1: Parameters of instrumentation tools.

Shaker	Laser	Acquisition PCI
Manufacturer: The Modal Shop Inc.	Manufacturer: Wenglor	Manufacturer: National Instruments
Model: K2004E01	Model: YP05MGVL80	Model: PCI-6229
Built-in Amplifier	Range: 43 to 53 mm (10 mm)	Analog Input: -10 V to 10 V
Gain 10 dB	Resolution: < 2 µm	Rate: 0.1 to 250000 scans/s
-	Output: 0 to 10 V	Analog Output: -10 V to 10 V
-	Scale: 1 V/mm	Rate: 0.1 to 833333.3 scans/s

4. EXPERIMENTAL PROCEDURE

Parameters like capacitance, anti-resonant and resonant frequency, damping ratio and mass are important to measure and estimate, for better model estimation and therefore, better harvest of energy. The first one is capacitance of the piezoelectric, C_P. This parameter is used to determine the GEMC and the modelling of equivalent electrical circuit.

As (Jordan & Langley, 2001) cited that capacitance may vary with frequencies and excitation amplitudes, but the standard capacitance measurement procedure is made using low electric tension amplitudes, scale of mV, and a fixed frequency of 1 kHz. Using a LCR meter of Agilent model E4980A, using long measurements for better accuracy.

To determine the frequencies, resonant and anti-resonant, a white noise was applied to shaker. The signal was Gaussian noise, filtered by a 4th order Butterworth low-pass and 100 Hz as cut-off frequency, estimated by a previous test. This test is applied with the PZT in short-circuit ($R_{load}=1\Omega$) and open circuit ($R_{load}=10M\Omega$).

The second method to estimate the resonant and anti-resonant frequency is making an impedance sweep in LCR, varying frequencies applied. An excitation electric tension amplitude must be set fixed, about 20 mV (same as used to determine the capacitance). The data acquisition was made with 400 Samples/s and 10^5 samples.

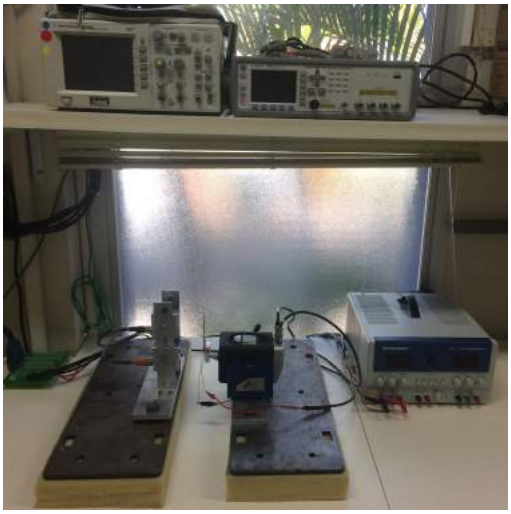

Figure 6: Mounting the workbench

After that, a Frequency Response Function (FRF) was calculated using a H_1 estimator, 50% overlap, windowed using Hanning and about 100 averages, like (Clementino, Marcel A.; Junior, Carlos D. M.; Silva, 2013) explained, and it is calculated to see the output response in function of input signal. The FRF curve is used to determine the damping factor (ξ) using a "3-dB down point technique", which consists of taking two sides frequencies about 3 dB above the peak in the log scale. In the Eq. 11, ω_n is the natural frequency estimated, ω_1 and ω_2 are the side frequencies with 3 dB less than ω_n.

$$\xi = \frac{\omega_2 - \omega_1}{2\omega_n} \tag{11}$$

The mass was measure using a precision electronic balances. The balance description is in Table 2.

The last part of experimental procedure is the modeling of system. Assuming the model presented in Fig. 2(b). A load (R_{load}) is connected to terminals and a current flow through it. A equation of V_{mc} in function of $I_{mc}(s)$ is:

$$sL_{mc}I_{mc}(s)+R_{mc}I_{mc}(s)+\frac{1}{sC_{mc}}I_{mc}(s)+\frac{R_{Load}}{sC_PR_{Load}+1}I_{mc}(s)=V_{mc}(s) \tag{12}$$

and considering that

$$V_P(s)=I_{mc}(s)\frac{R_{Load}}{sC_PR_{Load}+1} \tag{13}$$

So, the transfer function of V_P in function of V_{mc} in terms of s, is:

$$\frac{V_P(\boldsymbol{s})}{V_{mc}(\boldsymbol{s})}=\frac{sC_{mc}R_{Load}}{s^3(L_{mc}C_PR_{Load}C_{mc})+s^2(L_{mc}C_{mc}+R_{mc}C_PR_{Load}C_{mc})+s(R_{mc}C_{mc}+R_{Load}C_P+R_{Load}C_{mc})+1} \tag{14}$$

5. RESULTS

The capacitance was measured using, as said in the previous section, a LCR meter. Setting device to 20 mV of excitation amplitude and 1 kHz of frequency. It was obtained a value of 258,2148 nF.

An electronic balance was used to measure the mass of beam which results in 9,17g.

Next step is to measure the frequencies of open and shot-circuit. It can be measure using two methods. With the lasers to the beam's tip and coupled to the shaker, it can be estimate using the FRF of input signal and output signal, and using the LCR meter doing the impedance sweep, which consists in measure the impedance with different frequencies. In this work were made both tests. It can be seen in Figure 7(a) and (b), respectively.

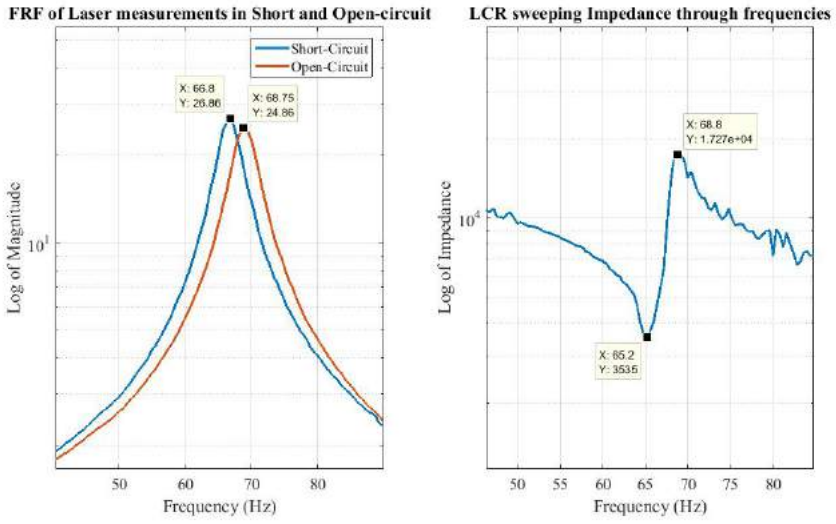

Figure 7: (a) FRF of input and output signal in short and open circuited mode and (b) Impedance sweeping through the frequencies.

Differences of results may be occurring due the precision of instruments and the difference of techniques used, other possible reason of differences are in the method, where FRF uses the mechanical displacement, while the LCR sweeping impedance uses electrical parameters.

To estimate the damping ratio, it was used the FRF of open-circuited, because the short-circuited is considered when $R_{load} = 0$, which is far from reality because there always will be a load at terminals. As previous explained, the damping ratio can be calculated using side frequencies below the resonant peak. The side frequencies are $\omega_1 = 419{,}716$ rad/s and $\omega_2 = 446{,}671$ rad/s, and the resonant frequency is $\omega_n = 431{,}969$ rad/s. Using Eq. 13, the damping ratio can be estimated as $\xi = 0{,}0312$.

To calculate the GEMC, it was used Eq. (4) and (6), and associating them (Hehn & Manoli, 2015).

$$\Gamma = \sqrt{m\,\omega_{SC}^2\,C_P\left(\frac{\omega_{OC}^2-\omega_{SC}^2}{\omega_{OC}^2}\right)} \tag{15}$$

For convenience was decided to use the frequencies measured by laser and calculated the FRF. Considering $\omega_{SC} = 419{,}716$ rad/s, $\omega_{OC} = 431{,}969$ rad/s, $m = 0{,}00917$ kg, $C_P = 258{,}215$ nF, and applying to Eq. (13), results a GEMC equals $\Gamma = 0{,}00483$.

The total damping and stiffness is calculated using the relations presented in (Hehn & Manoli, 2015), show in Eq. (14) and (15)

$$d = 2m\xi\omega_{SC} \tag{16}$$

$$k = m\omega_{SC}^2 \tag{17}$$

To build the model proposed in Fig. 2(b), it's necessary estimate the components. So, the parameters is $L_{mc} = 356{,}14\ H$, $R_{mc} = 9{,}32k\Omega$, $C_{mc} = 15{,}94nF$ and $V_{mc} = 15{,}32 * \sin(\omega t)$.

In order to validate the model, in Matlab® were made the simulation of system about the resonant characteristic. All the testes were made with amplitude acceleration of $5\ m/s^2$. The short and open circuit was tested with 1Ω and $10M\Omega$. Figure 9 show the model in relation of experimental.

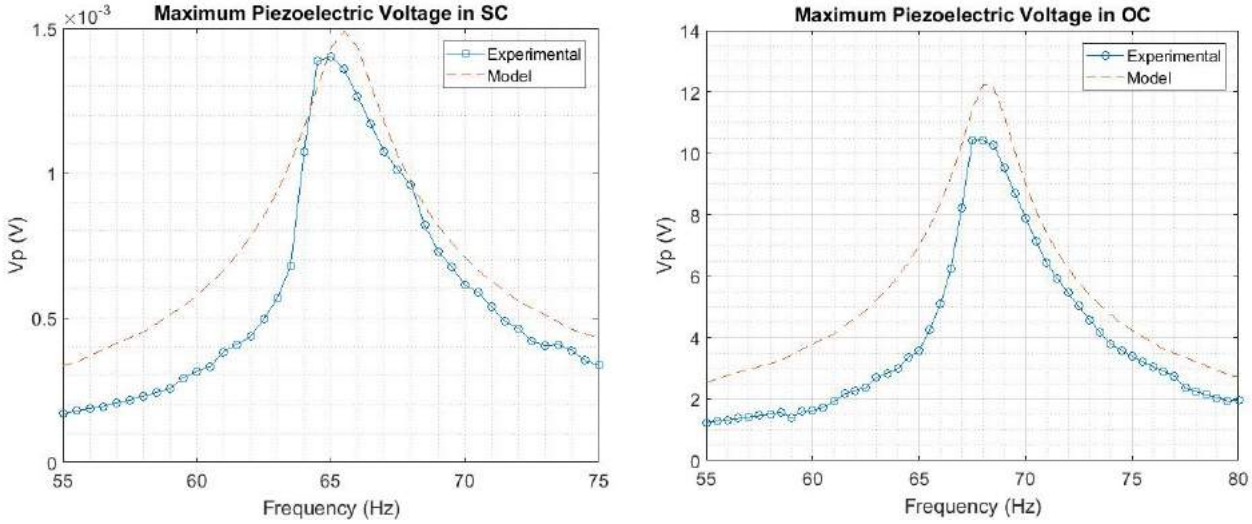

(a) (b)

Figure 8: Validation of model in piezoelectric voltage in Short-circuit (a) and Open-circuit (b)

After validating the model, the matching impedance is important to extract the maximum of energy available with a load. A curve of RMS power in function of load was traced as can be seen in figure 10. The maximum power available is P_{LIM} = 1,436 mW. And when an optimal resistance is applied as load, the optimal power is P_{RES} = 1,336 mW. The optimal load for this piezoelectric in resonant mode (f = 68 Hz) is 14kΩ for the simulation and the experimental is 8kΩ. The difference between the optimal resistance values presents a small deviation that can be explained by the imperfections of measurements.

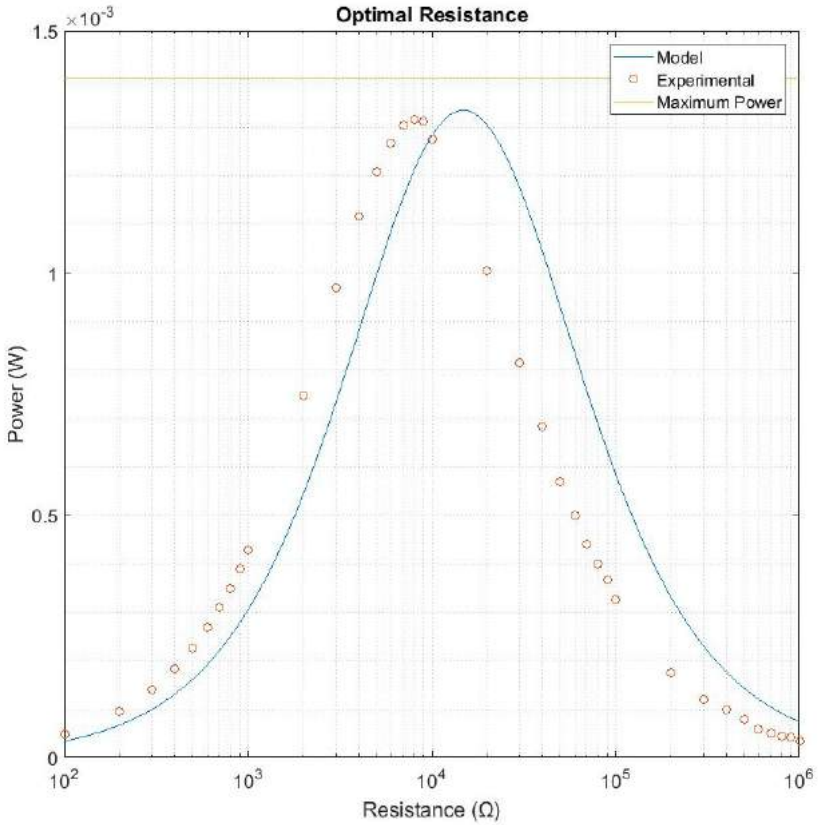

Figure 9: Maximum extractable power when resistance matching

6. CONCLUSION

This work presented a modelling of a beam with one degree-of-freedom to define the piezoelectric parameters. To execute the modelling was measured the resonant and anti-resonant frequencies from the mechanical displacement of beam's tip with laser sensors and LCR meter with impedance measurements, the capacitance using a LCR meter and the mass using a balance of precision. The others parameters were calculated from these values like the beam's stiffness and damping, the piezoelectric coupling factor, and finally an estimate of the maximum extractable power using different resistances. All the parameters were determined and calculated without any supplier information required, and using techniques that can be used for any structure containing piezoelectric devices.

The electric modelling was made considering all the elements of mechanical structure that the PZT is coupled. The validation of the model was proved with simulations and experimental tests. The response of the proposed model with different loads and frequencies were coherent with the experimental tests. This way, this model of harvester can be used for simulation and project of electronic interfaces based in rectifier circuits and switched converters. These systems are used for optimization of harvester's energy extraction, and for consumption/storage management in autonomous sensors.

7. ACKNOWLEDGEMENTS

This work was partial supported by CAPES with scholarship.

8. REFERENCES

Ajitsaria, J., Choe, S. Y., Shen, D., & Kim, D. J. (2007). Modeling and analysis of a bimorph piezoelectric cantilever beam for voltage generation. *Smart Materials and Structures*, *16*(2), 447–453. https://doi.org/10.1088/0964-1726/17/5/058001

APC International. (2011). *Piezoelectric Ceramics: Principles and Applications* (Second Edi). American Piezo Ceramics, Inc.

Clementino, Marcel A.; Junior, Carlos D. M.; Silva, S. (2013). Modeling of a Commercial Piezoelectric Energy Harvesting Device Through Experimental Identification, (Cobem), 3053–3064.

Clementino, M. A., Reginatto, R., & Da Silva, S. (2014). Modeling of piezoelectric energy harvesting considering the dependence of the rectifier circuit. *Journal of the Brazilian Society of Mechanical Sciences and Engineering*, *36*(2), 283–292. https://doi.org/10.1007/s40430-013-0070-6

Curie, J., & Curie, P. (1880). Développement, par pression, de l'électricité polaire dans les cristaux hémièdres à faces inclinées. *Comptes Rendus*, *91*, 294–295.

DuToit, N. E., Wardle, B. L., & Kim, S.-G. (2005). Design Considerations for Mems-Scale Piezoelectric Mechanical Vibration Energy Harvesters. *Integrated Ferroelectrics*, *71*(1), 121–160. https://doi.org/10.1080/10584580590964574

Erturk, A., & Inman, D. J. (2008). A Distributed Parameter Electromechanical Model for Cantilevered Piezoelectric Energy Harvesters. *Journal of Vibration and Acoustics*, *130*(4), 41002. https://doi.org/10.1115/1.2890402

Erturk, a., & Inman, D. J. (2008). On Mechanical Modeling of Cantilevered Piezoelectric Vibration Energy Harvesters. *Journal of Intelligent Material Systems and Structures*, *19*(11), 1311–1325. https://doi.org/10.1177/1045389X07085639

Giurgiutiu, V., Zagrai, a., & Jing Bao, J. (2002). Piezoelectric Wafer Embedded Active Sensors for Aging Aircraft Structural Health Monitoring. *Structural Health Monitoring*, *1*(1), 41–61. https://doi.org/10.1177/147592170200100104

Harb, A. (2011). Energy harvesting: State-of-the-art. *Renewable Energy*, *36*(10), 2641–2654. https://doi.org/10.1016/j.renene.2010.06.014

Hehn, T., & Manoli, Y. (2015). *CMOS Circuits for Piezoelectric Energy Harvesters - Efficient Power Extraction, Interface Modeling and Loss Analysis*. *Springer Series in Advanced Microelectronics* (Vol. 38). https://doi.org/10.1007/978-94-017-9288-2_2

Jordan, T. L., & Langley, N. (2001). NASA Piezoelectric Ceramics Characterization. *Contract*, 23.

Kim, H. S., Kim, J. H., & Kim, J. (2011). A review of piezoelectric energy harvesting based on vibration. *International Journal of Precision Engineering and Manufacturing*, *12*(6), 1129–1141. https://doi.org/10.1007/s12541-011-0151-3

Kong, N., Ha, D. S., Erturk, A., & Inman, D. J. (2010). Resistive Impedance Matching Circuit for Piezoelectric Energy Harvesting. *Journal of Intelligent Material Systems and Structures*, *21*(13), 1293–1302. https://doi.org/10.1177/1045389X09357971

Lallart, M., Garbuio, L., Petit, L., Richard, C., & Guyomar, D. (2008). Double synchronized switch harvesting (DSSH): A new energy harvesting scheme for efficient energy extraction. *IEEE Transactions on Ultrasonics, Ferroelectrics, and Frequency Control*, *55*(10), 2119–2130. https://doi.org/10.1109/TUFFC.912

Lynch, J. P., & Loh, K. J. (2006). A Summary Review of Wireless Sensors and Sensor Networks for Structural Health Monitoring. *The Shock and Vibration Digest*, *38*(2), 91–130. https://doi.org/10.1177/0583102406061499

Mason, T. O. (2011). Capacitor dielectric and piezoelectric ceramics. Retrieved August 2, 2017, from https://www.britannica.com/technology/capacitor-dielectric

Paula, A. S. De, & Barbosa, W. O. V. (2013). Experimental Investigation Investi Gation of Power Harvesting in a Mechanically Excited Piezoelectric Beam, (Cobem), 8386–8395.

Peairs, D. M., Park, G., & Inman, D. J. (2004). Improving Accessibility of the Impedance-Based Structural Health Monitoring Method. *Journal of Intelligent Material Systems and Structures*, *15*(2), 129–139. https://doi.org/10.1177/1045389X04039914

Ramadass, Y. K., & Chandrakasan, A. P. (2010). An efficient piezoelectric energy harvesting interface circuit using a bias-flip rectifier and shared inductor. *IEEE Journal of Solid-State Circuits*, *45*(1), 189–204. https://doi.org/10.1109/JSSC.2009.2034442

Renaud, M., Karakaya, K., Sterken, T., Fiorini, P., Van Hoof, C., & Puers, R. (2008). Fabrication, modelling and characterization of MEMS piezoelectric vibration harvesters. *Sensors and Actuators, A: Physical*, *145–146*(1–2), 380–386. https://doi.org/10.1016/j.sna.2007.11.005

Renaud, M., Sterken, T., Schmitz, A., Fiorini, P., Van Hoof, C., & Puers, R. (2007). Piezoelectric harvesters and MEMS technology: Fabrication, modeling and measurements. *TRANSDUCERS and EUROSENSORS '07 - 4th International Conference on Solid-State Sensors, Actuators and Microsystems*, 891–894. https://doi.org/10.1109/SENSOR.2007.4300274

Rupitsch, S. J., & Ilg, J. (2015). Complete Characterization of Piezoceramic Materials by Means of Two Block-Shaped Test Samples. *IEEE Transactions on Ultrasonics, Ferroelectrics, and Frequency Control*, *62*(7), 1403–1413.

Santos, A. A., Hobeck, J. D., & Inman, D. J. (2016). Analytical modeling of orthogonal spiral structures. *Smart Materials and Structures*. https://doi.org/10.1088/0964-1726/25/11/115017

Sazonov, E., Pillay, P., Li, H., & Curry, D. (2009). Self-Powered Sensors for Monitoring of Highway Bridges. *IEEE Sensors Journal*, *9*(11), 1422–1429. https://doi.org/10.1109/JSEN.2009.2019333

Vullers, R. J. M., van Schaijk, R., Doms, I., Van Hoof, C., & Mertens, R. (2009). Micropower energy harvesting. *Solid-State Electronics*, *53*(7), 684–693. https://doi.org/10.1016/j.sse.2008.12.011

Williams, C. B., & Yates, R. B. (1996). Analysis of a micro-electric generator for microsystems. *Sensors and Actuators A: Physical*, *52*(1–3), 8–11. https://doi.org/10.1016/0924-4247(96)80118-X

9. RESPONSIBILITY NOTICE

The authors are the only responsible for the printed material included in this paper.